

Neuronal Excitability

The Voltage-Gated Sodium Channel in *Drosophila*, Para, Localizes to Dendrites As Well As Axons in Mechanosensitive Chordotonal Neurons

Thomas A. Ravenscroft,^{1,2} Ashleigh Jacobs,³ Mingxue Gu,^{1,2} Daniel F. Eberl,³ and Hugo J. Bellen^{1,2,4}

<https://doi.org/10.1523/ENEURO.0105-23.2023>

¹Department of Human and Molecular Genetics, Baylor College of Medicine, Houston, TX 77030, ²Neurological Research Institute, Texas Children's Hospital, Houston, TX 77030, ³Department of Biology, University of Iowa, Iowa City, IA 52242, and ⁴Department of Neuroscience, Baylor College of Medicine, Houston, TX 77030

Abstract

The fruit fly *Drosophila melanogaster* has provided important insights into how sensory information is transduced by transient receptor potential (TRP) channels in the peripheral nervous system (PNS). However, TRP channels alone have not been able to completely model mechanosensitive transduction in mechanoreceptive chordotonal neurons (CNs). Here, we show that, in addition to TRP channels, the sole voltage-gated sodium channel (Na_v) in *Drosophila*, Para, is localized to the dendrites of CNs. Para is localized to the distal tip of the dendrites in all CNs, from embryos to adults, and is colocalized with the mechanosensitive TRP channels NompC and Inactive/Nanchung (Iav/Nan). Para localization also demarcates spike initiation zones (SIZs) in axons and the dendritic localization of Para is indicative of a likely dendritic SIZ in fly CNs. Para is not present in the dendrites of other peripheral sensory neurons. In both multipolar and bipolar neurons in the PNS, Para is present in a proximal region of the axon, comparable to the axonal initial segment (AIS) in vertebrates, 40–60 μm from the soma in multipolar neurons and 20–40 μm in bipolar neurons. Whole-cell reduction of *para* expression using RNAi in CNs of the adult Johnston's organ (JO) severely affects sound-evoked potentials (SEPs). However, the duality of Para localization in the CN dendrites and axons identifies a need to develop resources to study compartment-specific roles of proteins that will enable us to better understand Para's role in mechanosensitive transduction.

Key words: AIS; channel; mechanosensors; para; PNS; sodium

Significance Statement

Several transient receptor potential (TRP) channels have been shown to localize to dendrites of *Drosophila* mechanosensitive chordotonal neurons (CNs). Here, we show that the fly voltage-gated sodium channel (Na_v), Para, co-localizes with the TRP channels NompC and Iav and a possible dendritic spike initiation zone (SIZ) in CN dendrites. This dendritic localization is unique to CNs, is not seen in other peripheral neurons, and may account for some aspects of mechanotransduction. Para also localizes to a SIZ at an axonal initial segment (AIS)-like region, which is shared among many peripheral neurons.

Introduction

Animals need to sense their environment to move, find food, and avoid predators. Peripheral nervous system (PNS) neurons are responsible for detecting environmental cues

and relaying this information to the CNS. *Drosophila melanogaster* has provided important insights into sensory information processing in the PNS (Cosens and Manning, 1969; Göpfert et al., 2006; Akitake et al.,

Received March 27, 2023; accepted June 2, 2023; First published June 16, 2023.

The authors declare no competing financial interests.

Author contributions: T.A.R., A.J., D.F.E., and H.J.B. designed research; T.A.R., A.J., M.G., and D.F.E. performed research; T.A.R., A.J., M.G., D.F.E., and H.J.B. analyzed data; T.A.R., A.J., M.G., D.F.E., and H.J.B. wrote the paper.

2015). The fly PNS contains multipolar and bipolar neurons (Bodmer and Jan, 1987; Orgogozo and Grueber, 2005). Multipolar neurons have one axonal neurite and many dendrites (Grueber et al., 2001; X. Wang et al., 2015). The expansive dendritic tree provides broad coverage of the animals' periphery where transient receptor potential (TRP) channels open in response to pain, touch, and heat stimuli (Liu et al., 2003; Tracey et al., 2003; Zhong et al., 2010; Tsubouchi et al., 2012). Bipolar neurons have one axon and one dendrite separated by the soma (Orgogozo and Grueber, 2005). Bipolar neurons contain TRP channels sensitive to odors, chemicals, light, stretch, and sound (Stocker, 1994; Carlson et al., 1997; Vervoort et al., 1997; Ainsley et al., 2003; Schrader and Merritt, 2007; Suslak et al., 2015), and the singular dendrite enables the animal to precisely locate the direction of both attracting and deterring stimuli. Therefore, the TRP channel composition and orientation of neurons in the *Drosophila* PNS are optimized for sensing directional stimuli.

TRP channels alone do not account for all the electrophysiological properties of all sensory neuron dendrites. In *Drosophila*, a null allele for the mechanosensitive TRP channel *No mechanical potential C* (*NompC*), which is localized to the most distal region of CN dendrites (Cheng et al., 2010; J. Lee et al., 2010), still has mechanosensitive properties in CNs (Eberl et al., 2000; Zhang et al., 2013). In addition to *NompC*, *Drosophila* CN dendrites also contain the TRP channels inactive (*lav*) and nanchung (*Nan*) which form a functional heterodimer (Gong et al., 2004). Unlike *NompC*, *Nan* and *lav* are required for the mechanosensitive response, however, in S2 cells the *Nan-lav* complex alone is not mechanosensitive (B. Li et al., 2021). Hence, it is likely that not all the ion channels responsible for mechanotransduction in *Drosophila* are known.

In another invertebrate, the crayfish *Astacus astacus*, a model of the mechanosensitive response in stretch receptors using just TRP channels was unable to recapitulate *in vivo* recordings (Swerup and Rydqvist, 1996). However, when the models were altered to incorporate voltage gated sodium (Na_v) channels, the recordings matched *in vivo* recordings indicating a possible mechanosensation role for Na_v channels (Suslak et al., 2011). Additionally, electrical spikes are present in mechanosensitive locust auditory neuron dendrites (Hill, 1983; Warren and Matheson, 2018) which are similar to the chordotonal neurons (CNs) in the Johnston's organ (JO) in *Drosophila*. These spikes occur in the distal region of the dendrite and are sensitive to

tetrodotoxin (TTX) suggesting a role for Na_v channels in mechanosensitive neurons (Hill, 1983; Warren and Matheson, 2018). Together this shows that mechanosensation in invertebrates does not just rely on mechanosensitive TRP channels and that Na_v channels may play a role in some peripheral neurons.

Drosophila has one Na_v channel gene encoded by *paralytic* (*para*; Suzuki et al., 1971). In the unipolar neurons of the CNS, *para* is expressed in active, mature neurons and is localized to the spike initiation zone (SIZ), where action potentials are generated (AP), at a distal axonal segment (DAS; Ravenscroft et al., 2020). Little is known about *Para* distribution in the multipolar and bipolar neurons of the PNS. Gene expression reporters in late embryos reveal *para* is expressed in some PNS neurons but it is unclear whether it is expressed in all or only some neurons (Hong and Ganetzky, 1994; Ravenscroft et al., 2020).

To determine the role of Na_v channels in mechanosensation in the *Drosophila* PNS we used a previously generated *Minos*-mediated integration cassette (MiMIC) protein trap inserted into the *para* locus to identify the distribution of *Para* (Venken et al., 2011; Lee et al., 2018; Ravenscroft et al., 2020). Using this allele, we identified the axonal SIZ of multidendritic and bipolar CNs in the third instar larval PNS in an axonal initial segment (AIS)-like region. Interestingly, we observe *Para* at the distal dendritic tip of all CN dendrites throughout development, indicating another role for Na_v channels in the peripheral mechanical response.

Materials and Methods

Fly lines and maintenance

Flies were raised on a standard molasses-based lab diet at 22°C in constant light conditions. All crosses were performed at 25°C in a 12-h light/dark incubator. Animals were not selected for sex at embryonic, larval, or pupal stages. Fly lines used are listed in Table 1. All fly lines used are either deposited in Bloomington *Drosophila* Stock Center, the Vienna *Drosophila* Resource Center, or are available on request. The characterization and validation of the gene-trap and protein-trap *para*-alleles were previously performed by Ravenscroft et al., 2020.

Immunostaining

Embryos

Immunostaining of *Drosophila* embryos was done as described previously (Rothwell and Sullivan, 2007). Flies were crossed in a chamber containing a grape juice plate (Welch) at 22°C in constant light. Flies lay eggs predominantly around dusk; therefore, to collect embryos at stage 16 we waited for 20–24 h for collection. Embryos were collected with a paintbrush and water into a cell collection chamber (VWR #732–2758). These baskets were placed in a 50% bleach solution for dechoriation and agitated with a pipette. Dechoriation was observed under a microscope and once >75% of embryos lost the dorsal appendages the embryos were washed with an embryo wash solution (0.7% NaCl, 0.05% Triton X-100 in water). The basket was then dried by placing the chamber on a Kim wipe. For fixation, the mesh of the basket was removed

T.A.R. was supported by The Cullen Foundation. D.F.E. and A.J. were supported in part by the National Science Foundation Grant 2037828. A.J. was supported in part by a University of Iowa Center for Research by Undergraduates Fellowship. H.J.B. was supported by the Howard Hughes Medical Institute.

Acknowledgments: D.F.E. thanks Jason Caldwell for preliminary RNAi experiments. We thank Changsoo Kim for the *lav*-GFP flies and Yuh-Nung Jan for the *NompC* antibody. Figures 4A, 5E, and 6C were created with biorender.com by T.A.R.

Correspondence should be addressed to Hugo J. Bellen at hbellen@bcm.edu.

<https://doi.org/10.1523/ENEURO.0105-23.2023>

Copyright © 2023 Ravenscroft et al.

This is an open-access article distributed under the terms of the Creative Commons Attribution 4.0 International license, which permits unrestricted use, distribution and reproduction in any medium provided that the original work is properly attributed.

Table 1: Summary of fly lines used in this study

Fly line	Genotype	Stock source	Reference
<i>para-GFP</i>	$y^1 w^{67c23} paraMI08578-GFSTF.0 Mi\{PT-GFSTF.0\}MI08578a Mi\{PT-GFSTF.0\}MI08578b$	BDSC #91528	Ravenscroft et al. (2020)
<i>para-RFP</i>	$y^1 w^{67c23} paraMI08578-TRH.0 Mi\{PT-TRH.0\}MI08578a Mi\{PT-TRH.0\}MI08578b$	BDSC #92157	Ravenscroft et al. (2020)
<i>Para-T2A-GAL4</i>	$y^1 w^{67c23} Mi\{Trojan-GAL4.0\}paraMI08578-TG4.0/FM7c$	BDSC #91527	Ravenscroft et al. (2020)
<i>221-GAL4</i>	$w^*; Pin^1/CyO; P\{?GawB\}221w-$	BDSC #26259	J. Huang et al. (2008)
<i>tilB-GAL4, nan-GAL4</i>	$w^{1118}; tilB-Gal4 nan-Gal4$		Kim et al. (2003); Kavlie et al. (2010)
<i>nompB-GAL4</i>	$w^{1118}; PBac\{IT.GAL4\}nompB2151-G4/CyO$	BDSC #65724	Gohl et al. (2011)
<i>ato-GAL4</i>	$y^1 w^*; P\{ato-GAL4.3.6\}10$	BDSC #9494	Hassan et al. (2000)
<i>UAS-RedStinger</i>	$w^*; P\{w[+mC]=UAS-RedStinger\}4, P\{w[+mC]=UAS-FLP.D\}JD1, P\{w[+mC]=Ubi-p63E(FRT.STOP)Stinger\}9F6/CyO$	BDSC #28280	Evans et al. (2009)
<i>UAS-mCD8::RFP</i>	$w^*; P\{y[+t7.7] w[+mC]=10 \times UAS-IVS-mCD8::RFP\}attP40$	BDSC #32219	Pfeiffer et al. (2010)
<i>UAS-mCherry</i>	$y^1 w^*; wg\{Sp-1\}/CyO, P\{Wee-P.ph0\}Bacc[Wee-P20]; P\{y[+t7.7] w[+mC]=20 \times UAS-6 \times mCherry-HA\}attP2$	BDSC #52268	Shearin et al. (2014)
<i>UAS-para-RNAi-GD3392</i>	$w^{1118}; P\{GD3392\}v6131$	VDRC #6131	Dietzl et al. (2007)
<i>UAS-para-RNAi-GD3392</i>	$w^{1118}; P\{GD3392\}v6132$	VDRC #6131	Dietzl et al. (2007)
<i>UAS-para-RNAi-KK108534</i>	$P\{KK108534\}VIE-260B$	VDRC #104775	Dietzl et al. (2007)
<i>UAS-Dicer2</i>	$w^{1118}; P\{w[+mC]=UAS-Dcr-2.D\}10$	BDSC # 24651	Dietzl et al. (2007)
Canton S	Canton-S	BDSC # 64349	

with a razor blade and placed in a glass scintillation vial. The mesh was washed with 1 ml of heptane saturated with 37% formaldehyde (equal volumes of heptane and 37% formaldehyde were placed in a scintillation vial and vigorously mixed several times, the solution was allowed to settle into two phases with saturated heptane in the upper phase) which removed the embryos from the mesh. The mesh was then removed and 1 ml of 3.7% formaldehyde in PEM buffer (0.1 M PIPES, 1 mM MgCl₂, and 1 mM EGTA, pH 6.9, in water) was added, the vial was vigorously mixed for 15 s, and then left at room temperature for 20 min. The bottom formaldehyde layer was then removed and replaced with methanol (100%), this mixture was vigorously mixed for 15 s and left to stand for 1 min. After the embryos sank to the bottom of the vial and the upper heptane layer was removed. The vial was then filled ~2/3 full of 100% methanol and left to sit at 4°C overnight. Embryos were then transported to a 1.5 ml Eppendorf tube. As much methanol as possible was removed and replaced with 500 μl of PBTA (1 × PBS, 0.05% Triton X-100, 0.02% sodium azide). They were then placed on a rotator at room temperature for 15 min to rehydrate. Primary antibodies were then incubated in the vials in PBTA and left at 4°C overnight on a rotator. Antibodies were then recovered, and embryos were rinsed three times with PBTA and left for 1 h in PBTA on a rotator. Secondary antibodies were then added in PBTA and incubated on a rotator at room temperature for 2 h (wrapped in foil to avoid light exposure). Antibodies were then recovered, and embryos were rinsed three times with PBTA and left for 1 h in PBTA on a rotator. Embryos were rinsed four times with PBS-Azide (1 × PBS, 0.02% sodium azide) to remove the detergent. Embryos were mounted in rapiclear 1.47 (SUNjin labs) for imaging. Embryos were mounted on a glass slide with a coverslip with no spacer.

Antibodies used were rabbit-GFP 1:200 (Invitrogen #A-11122), rat-Elav 1:500 (DSHB #7E8A10), mouse-FLAG 1:200 (F3165 Sigma), rabbit-NompA 1:200 (Chung et al., 2001). Secondary antibodies used were goat-anti-HRP-Cy3 1:500 (Jackson ImmunoResearch, #123-165-021) and corresponding donkey secondary antibodies 1:500 (Jackson ImmunoResearch).

Third instar larvae

Wandering third instar larvae were placed in cold 1 × Schneiders medium (SM). Larvae were pinned on a Sylgard plate with Minuten pins in the anterior and posterior of the animal, dorsal side down. An incision was made with fine dissection scissors from the posterior to the anterior of the animal. Internal organs and fat were removed from the animal. Pins were placed to fillet the larvae. Three to four animals at a time were filleted on each plate. The SM was then replaced with 3.7% paraformaldehyde (PFA) in SM and placed on a gentle rocker for 20 min at room temperature. After 20 min larvae were rinsed three times with SM, pins were removed and larvae were placed in a micro-Eppendorf tube in 0.1% PBS-TX (1 × PBS, 0.1% Triton 100-X), tubes were washed three times for 10 min on a rotator at room temperature. Primary antibodies were then added and incubated with 0.1% PBS-TX overnight on a rotator at 4°C. Antibodies were then recovered, and animals were rinsed three times with 0.1% PBS-TX and then washed three times for 10 min in 0.1% PBS-TX. Secondary antibodies were then added and incubated (wrapped in foil) for 2 h at room temperature on a rotator. Antibodies were then recovered, and animals were rinsed three times with 0.1% PBS-TX and then washed three times for 10 min in 0.1% PBS-TX. Larvae were then mounted on a glass slide in rapiclear 1.47 (SUNjin labs)

under a coverslip with no spacer. Antibodies used were rabbit-GFP 1:200 (Invitrogen #A-11122), mouse-GFP 1:200 (Sigma G6539), rabbit-NompA 1:500 (Chung et al., 2001), mouse-Eys 1:50 (DSHB #21A6 (Fujita et al., 1982)), and rabbit-NompC 1:300 (Cheng et al., 2010). Secondary antibodies used were goat-anti-HRP-Cy3 1:500 (Jackson ImmunoResearch, #123-165-021) and corresponding donkey secondary antibodies 1:500 (Jackson ImmunoResearch). The specificity of the anti-GFP antibody for Para-GFP is shown in Extended Data Figure 4-1.

Intensity profiles for Para distribution were calculated using a previously published approach (Jegla et al., 2016). Stacked confocal images of *ddaE* neurons were processed in ImageJ, a line was measured from the soma along the axon as far as a single axon track could be followed. The intensity of UAS-mCherry and GFP staining was recorded using the measurement feature. Relative intensity was measured by dividing the measured value by the average of the lowest 20% of measurements. This value was then divided by the top 5% of values (after dividing by the lowest 20%) to give a relative intensity. This was performed on $n=15$ neurons from $n=5$ animals. Measurements from all animals were then combined, smoothed out to an average of 50 values, and plotted on a graph. GFP to mCherry ratio was measured by comparing each relative GFP measurement to the corresponding mCherry measurement. For CN neurons the measurements were started at the distal tip of the dendrite through the soma into the axon. These data were represented with the soma at 0 using the max intensity point of *mCD8::mCherry* as the soma. Because of variation in dendrite length between animals, a representative trace is shown.

Johnston's organ. Johnston's organ dissections and imaging were performed as described previously (T. Li et al., 2016). Pupae 24–48 h after puparium formation were placed on double-sided tape on a glass slide. Using forceps, the outer shell was removed, and the pupae were removed and placed in a Sylgard dish in SM. Using micro scissors, the head was removed. A pipette was used to provide suction and remove the fat and the brain from the head, leaving the antenna attached to the outer membrane. This membrane was fixed in 3.7% PFA in PBS for 20 min, then rinsed three times and washed three times for 10 min in 0.1% PBS-TX. Samples were incubated in conjugated antibodies in 0.1% PBS-TX and incubated overnight at 4°C. Antibodies were recovered and samples were rinsed three times and washed three times for 10 min in 0.1% PBS-TX. Samples were mounted in Vectashield on a glass slide with 2 pieces of double-sided tape acting as a spacer to protect the antennae. Antibodies used were rabbit-GFP-488 1:200 (Invitrogen), and goat-phalloidin-Cy3 1:500 (Jackson ImmunoResearch).

Johnston's organ electrophysiology

Sound-evoked potential (SEP) recordings were performed with an electrolytically sharpened tungsten recording electrode inserted into the joint between antennal segments one and two, and a reference electrode inserted into the head cuticle near the posterior orbital bristle, in response to near-field playback of computer-generated pulse

song (described by Eberl and Kernan, 2011). The signals were subtracted and amplified with a differential amplifier (DAM50, World Precision Instruments) and digitized at 10 kHz (USB-6001, National Instruments). Average response values were measured as the max-min values in an averaged trace from 10 consecutive presentations of the described protocol.

Experimental design

All confocal images of embryos were correctly aged using the structure of the CNS labeled by horseradish peroxidase (HRP). JO images were taken from pupae 48–72 h after puparium formation. Adult flies aged 2–7 d were used for JO electrophysiology. Images from more than five animals for each condition were obtained.

Statistical analysis

A one-way analysis of variance (ANOVA) with Brown-Forsythe correction for unequal standard deviations was used for the comparison of SEP in JO electrophysiology data. Graphs indicate, within each bar, the number of antennae tested for that genotype. Statistical significance depicted on graphs indicate Tukey's *post hoc* multiple comparisons test.

Results

para is expressed in multidendritic neurons and CNS in *Drosophila* embryos

para expression is first noted at stage 16 of embryonic development where it is expressed in some CNS neurons (Hong and Ganetzky, 1994; Ravenscroft et al., 2020). The *para-T2A-GAL4* allele, when paired with a fluorescent reporter (*UAS-mCD8::GFP*), labels the cells that express *para* (Ravenscroft et al., 2020). We used *para-T2A-GAL4* to determine the expression pattern of *para* in the PNS in stage 16 embryos. The PNS of embryos contains developing multipolar and bipolar neurons responsible for mechanosensation, proprioception, temperature, and touch (Orgogozo and Grueber, 2005). Multipolar neuron cell bodies have multiple dendritic processes with one axon, whereas bipolar neuron cell bodies have only one dendrite and one axon. These neurons can be easily identified by their location on the embryo (Singhania and Grueber, 2014): the dorsal cluster of neurons (Fig. 1A, box ii) are all multipolar, a medial cluster of 5 neurons lined up parallel to each other are bipolar lateral chordotonal neurons (*lch5*; Fig. 1A, box i). Like in the CNS (Ravenscroft et al., 2020), *para* is not expressed in all PNS neurons (Fig. 1A) as *para* is expressed in a restricted number of multipolar neurons (Fig. 1A, box i). Unlike the multipolar neurons, *para* is expressed in all the bipolar CNs (Fig. 1A, box ii). Note that muscle cells in the embryo are also not labeled with *para*, in contrast to vertebrates where Na_v channels are needed for muscle contraction (George et al., 1991).

Para is localized to embryonic CN dendrites and soma

To determine Para localization, a MiMIC converted *para*-allele containing multiple epitopes for antibody labeling

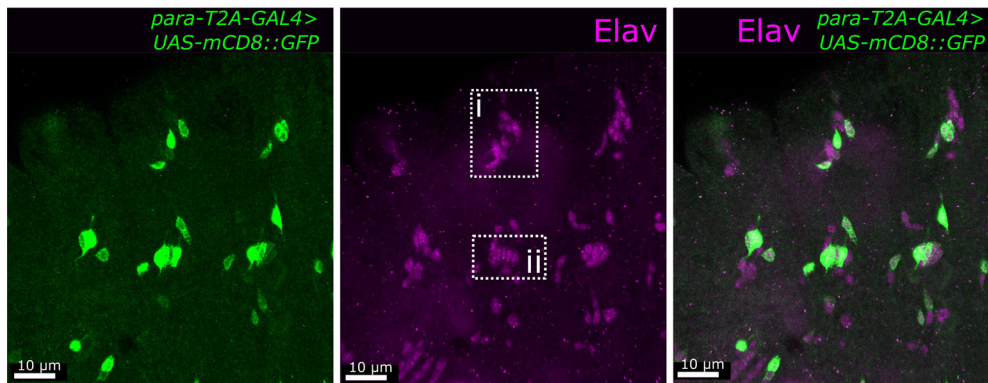


Figure 1. *para* is expressed in embryonic chordotonal neurons. The *para-T2A-GAL4* allele combined with a *UAS-mCD8::GFP* enables the visualization of *para*-expressing cells. In stage 16 embryos, where *para* is first expressed, *para* is expressed in a restricted number of Elav-positive PNS neurons including all chordotonal neurons (box i), *para* is expressed in some multidendritic neurons (box ii).

[Para-GFP-FIASH-Strep-TEV-FLAG (further referred to as Para-GFP)] was used (Venken et al., 2011; Ravenscroft et al., 2020). The Para-GFP allele has been previously validated and characterized to be representative of endogenous Para localization (Ravenscroft et al., 2020). We tested where Para is localized in the neurons relative to Elav, which marks the soma of neurons, and HRP, which labels all neuron membranes.

In stage 16 embryonic multidendritic neurons, Para-GFP is not observed in the axons, dendrites, or soma (Fig. 2A). At this stage the multidendritic neurons are still developing (Bodmer and Jan, 1987; Hartenstein, 1988); however, unlike the developing motor neurons of the CNS where Para is localized to the soma (Ravenscroft et al., 2020), Para is not detected in multidendritic neurons during development. This indicates Para's functional role in these neurons occurs at later stages of development. In contrast, CNs become fully differentiated in stage 16 of embryonic development (Jarman et al., 1993). *para* is strongly expressed in all embryonic CNs at stage 16. Para is predominantly localized to the distal tip of the dendrites with a lower level of Para seen in the soma (Fig. 2B). Super-resolution stimulated emission depletion (STED) microscopy revealed that Para is present at the very distal tip of the dendrite with no membrane labeling via HRP present beyond where Para is localized (Fig. 2C). No Para is detected in the axon at this stage. The distal tip of the CN dendrite is connected to a dendritic cap via an extracellular matrix (ECM) that includes the glycoprotein NompA. NompA is specifically expressed in type I sense organs by support cells (scolopale cells) that ensheath the sensory process (Chung et al., 2001). In the distal CN dendrite of stage 16 embryos, Para is surrounded by NompA (Fig. 2D).

Para is expressed in all PNS neurons in third instar larvae and enriched at an AIS-like region in axons of multipolar neurons

We assessed the expression pattern in the third instar larval stage using *para-T2A-GAL4*. *para-T2A-GAL4* expression of *UAS-nls.mCherry* (Evans et al., 2009) shows that *para* is expressed in all Elav-positive neurons in the PNS (Fig. 3A). This contrasts with the expression of *para*

in the third instar larvae CNS where it is only present in ~25% of neurons (Ravenscroft et al., 2020).

In the third instar larva and adult CNS Para is localized to a DAS while in stage 16 embryos Para is localized to the soma of neurons (Ravenscroft et al., 2020). Most CNS neurons in *Drosophila* are unipolar, while PNS neurons are either multipolar (multidendritic neurons) or bipolar (CNs). To determine Para localization in fully developed PNS neurons we used Para-GFP in combination with 221-GAL4 (Huang et al., 2008), which drives GAL4 expression in some multipolar PNS neurons including ventral dendritic arborization (vpda) and dorsal dendritic arborization (ddaE) neurons (Grueber et al., 2003), and *UAS-mCherry* (Shearin et al., 2014) in wandering third instar larva. In both the multidendritic vpda (Fig. 3B) and ddaE neurons (Fig. 3C), like CNS neurons, Para is localized to the axon but not the soma or dendrites. However, unlike in the CNS, Para is enriched in a segment that is only 40–60 μm from the soma (Fig. 3D). This region overlaps with a previously reported AIS-like region marked by the localization of overexpressed Ankyrin 2 (Ank2) isoforms but is distal to the localization of overexpressed voltage-gated potassium (K_v) channels Eag-like K^+ channel (Elk) and Shaker cognate I (Shal) (Jegla et al., 2016). Beyond the AIS-like region, Para is still present at lower levels. We speculate that continued Para distribution is needed to maintain AP propagation beyond the initiation site. Additionally, in the vpda neuron, we observe dendrites that enter the axons beyond the cell body (Fig. 3B). This branching has been previously reported to occur in some vpda neurons (Schrader and Merritt, 2000). Similar to Para localization at a DAS in CNS neurons, Para is localized distal to the axonal dendrite in the vpda neurons.

In the larva, PNS Para is localized to axons and dendrites of CNs

CNs are part of a four-cell chordotonal organ containing a neuron, a ligament cell that anchors the neurons, a cap cell that is attached to the CN dendrite via the dendritic cap, and a scolopale cell that protects and maintains the environment around the CN dendrite (Fig. 4A; Hartenstein, 1988). CN neurons and dendrites, like multidendritic neurons, continue

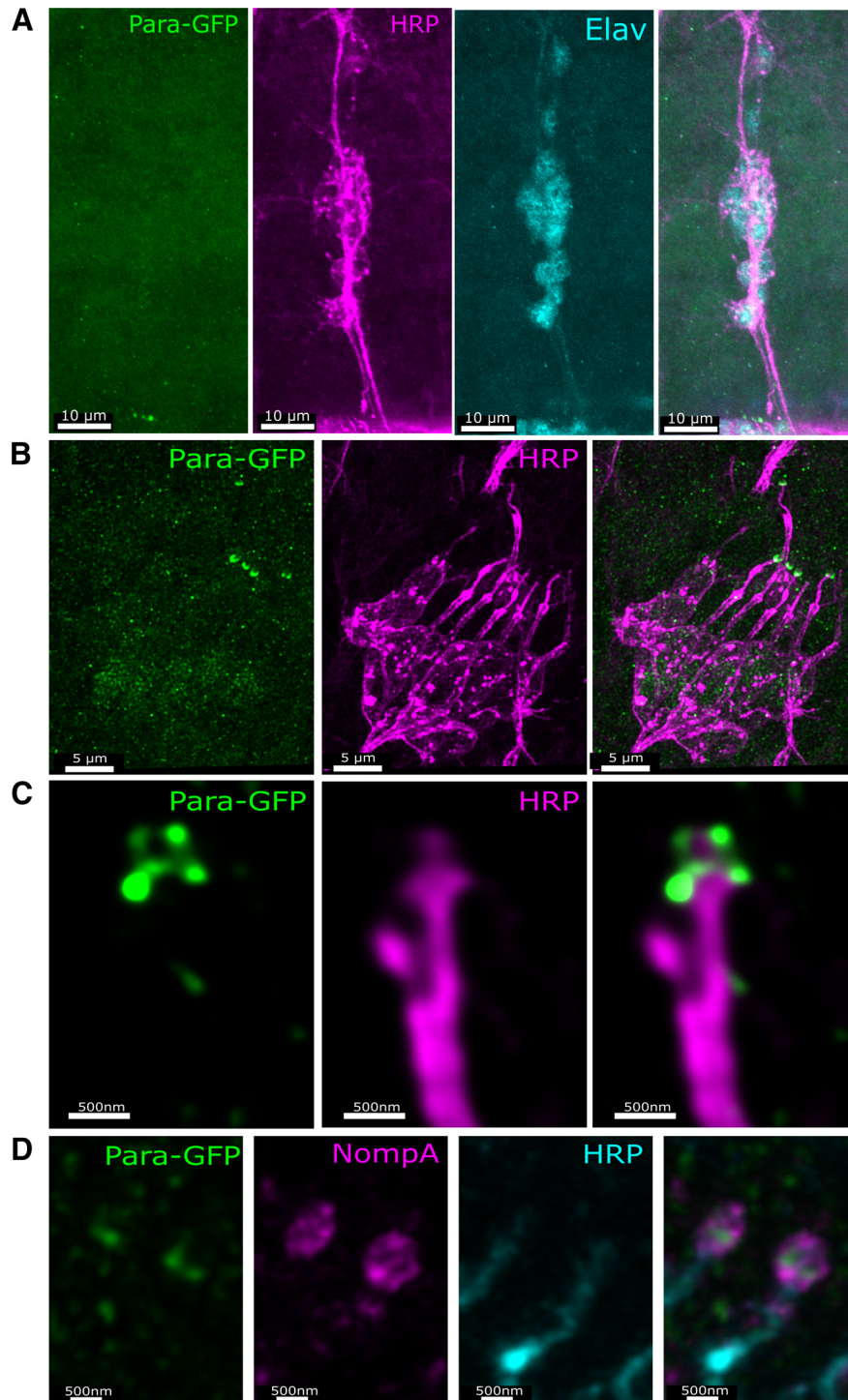


Figure 2. Para is enriched in the distal dendrites of embryonic chordotonal neurons. Despite *para* expression in multidendritic neurons (Fig. 1), the Para protein cannot be seen in axons, the soma, or dendrites indicating expression is very low (A). In the chordotonal neurons, Para is seen predominantly in the dendrites with less Para in the soma and no observed Para in axons. Neuronal membranes are labeled with an antibody against horseradish peroxidase (HRP; B). Para is localized to the very distal tip of the dendrite (C), where it is surrounded by the dendritic cap protein NompA (D).

to stretch and grow as the larvae grow (Singhania and Grueber, 2014). In wandering third instar larvae, the CNs reach their maximum length. In the *lch5* CNs in the larval abdomen, Para is enriched in axons (Fig. 4B). As in multidendritic

neurons, Para in CNs is localized in the proximal part of the axon but unlike multidendritic neurons, Para is enriched close to the soma (20–30 μm; Fig. 4D). Additionally, the drop-off in the intensity of Para

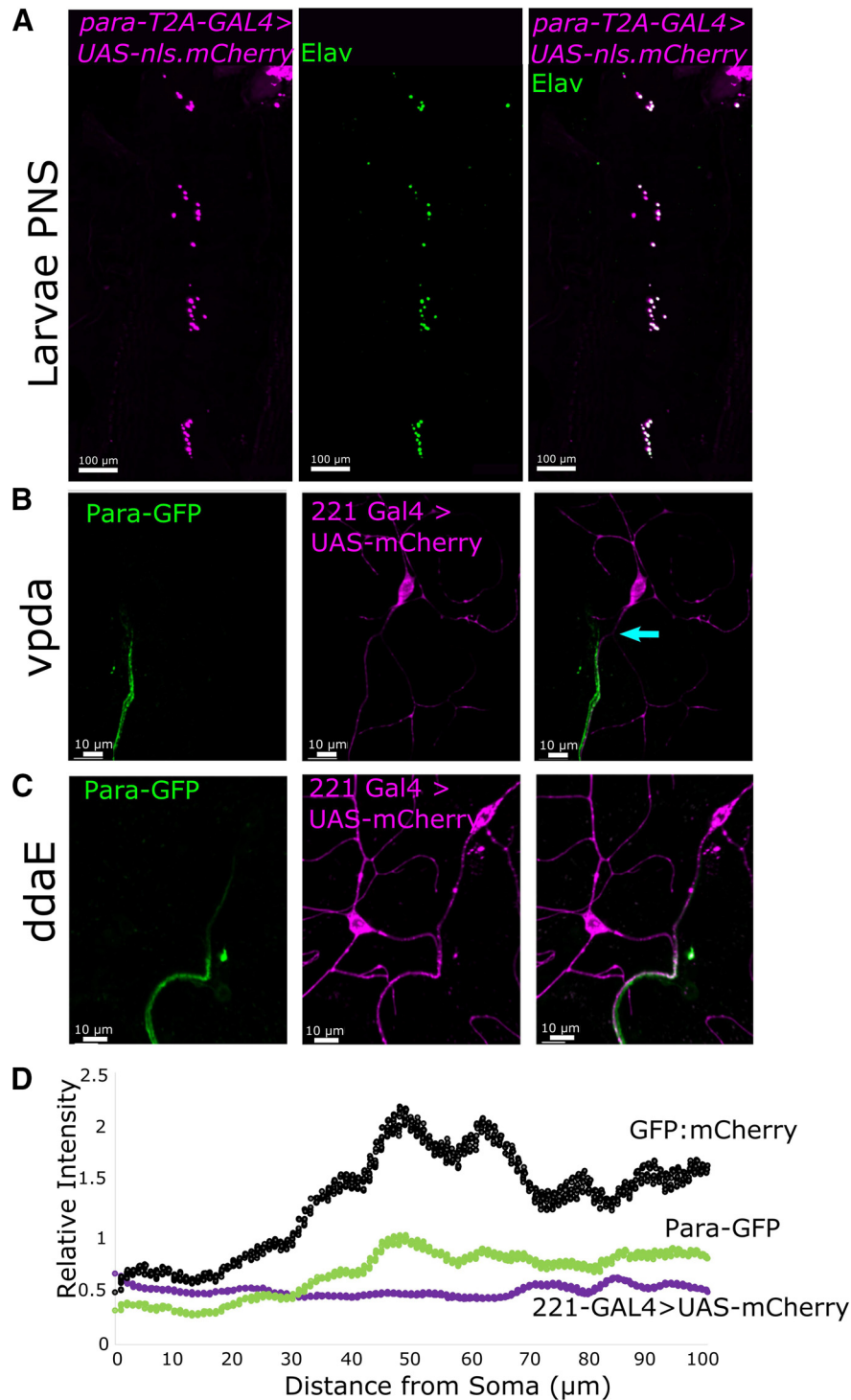


Figure 3. Para is localized to an AIS-like region in multipolar neurons of the third instar larvae PNS. *para* is essential for larval development and hence the expression and localization of Para in larval stages likely indicate where it functions. In the third instar larvae, PNS *para* is expressed in all neurons (Elav-positive cells; **A**). In the third instar larvae multidendritic PNS neurons, Para is localized to the proximal axon in both *vpda* (**B**) and *ddaE* (**C**) neurons. In *vpda* neurons, a dendrite can be seen in the proximal axon (arrow), Para is localized distal to this dendrite. In *ddaE* neurons, the relative intensity of Para localization is highest $\sim 40\text{--}60\ \mu\text{m}$ from the soma indicating the presence of an axonal initial segment-like region in the third instar larva PNS (**D**). Beyond the AIS-like region, Para is still present at lower levels, likely to maintain the propagation of depolarizations to the synapse.

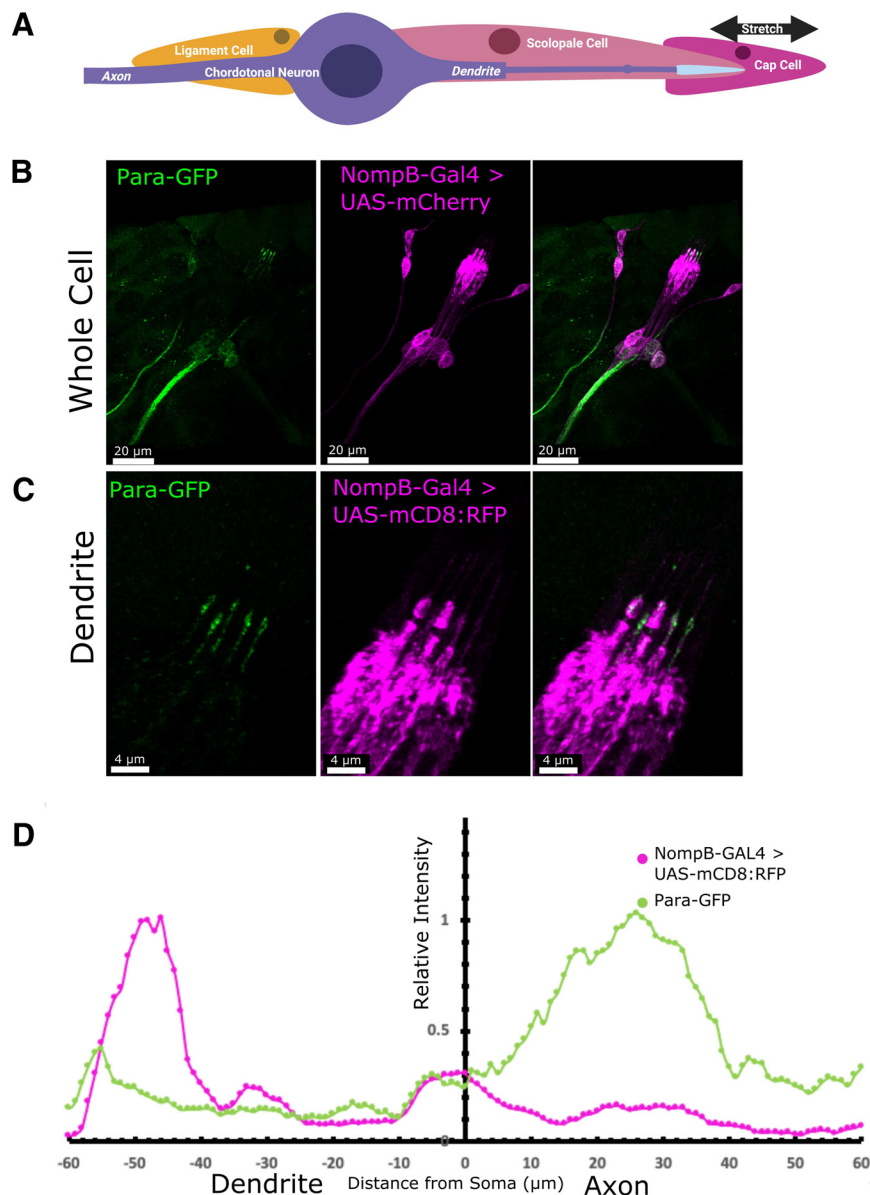


Figure 4. Para is localized to both axons and dendrites in third instar larval chordotonal neurons. The chordotonal neuron is part of a 4-cell chordotonal organ (**A**). The neuron is anchored at the soma by a ligament cell and at the dendrite by the cap cell. The dendrite is insulated by a scolopale cell that provides structural support and protects the ionic balance of the dendritic space. NompB-GAL4 is expressed in the chordotonal neurons of the third instar larval PNS (Gohl et al., 2011) and with UAS-mCD8::RFP (Pfeiffer et al., 2010) these neurons can be visualized (**B**). Para is enriched in both the axon and dendrite of the lch5 neuron (**B**). In the axon, Para is localized $\sim 20\text{--}30\ \mu\text{m}$ proximal to the soma, closer than what is observed in multidendritic neurons (**D**). In the dendrites (**C**), Para is localized to the distal dendrite $\sim 50\text{--}60\ \mu\text{m}$ from the soma (**D**). The distance on the axis in **D** indicates the distance from the soma into the dendrite (0 to $-80\ \mu\text{m}$) and the axon (0 to $+80\ \mu\text{m}$). The specificity of the anti-GFP for Para-GFP is shown in Extended Data Figure 4-1.

localization beyond the AIS-like region is greater in the CNs than in the multidendritic neurons. Hence, the AIS-like region is present in bipolar PNS cells as well as multipolar cells.

In the dendrites of the third instar larval lch5 CNs, like in embryonic CNs, Para is localized to the distal tip (Fig. 4C). Para is less abundant at the dendrite than it is at the axon (Fig. 4D). When compared with the localization of the cap protein NompA (Chung et al., 2001), Para is enriched both distal and proximal to the cap (Fig. 5A). The more proximal localization of Para overlaps with the

ciliary dilation which can be seen by the expansion of the dendrite distal to the extracellular scaffolding protein eyes-shut (Eys; Fig. 5B; Blochlinger et al., 1991; Husain et al., 2006). Low levels of Para can also be seen proximal to the ciliary dilation. The dendrites of the CNs contain the mechanosensitive ion channels NompC, and the two interdependent TRP channels lav and Nan (Nan; Zhang et al., 2013). NompC is localized at the ciliary dilation and at the tip of the dendrite, while lav and Nan are localized proximal to the ciliary dilation (Fig. 5E; Gong et al., 2004; J. Lee et al., 2010; Liang et al., 2011). Para

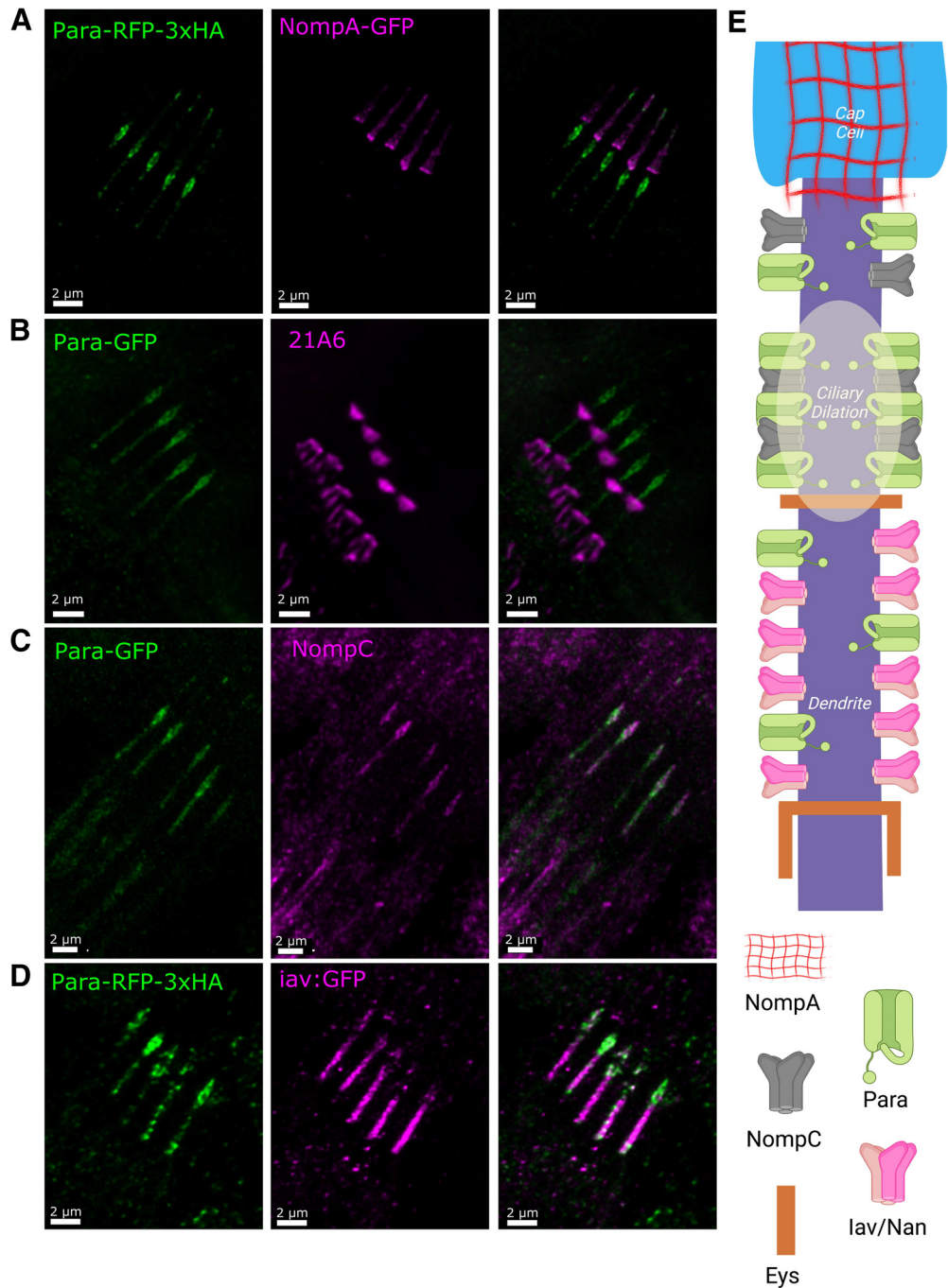


Figure 5. Para colocalizes with NompC in the ciliary dilation and distal dendrite of third instar larva chordotonal neurons. Several proteins have been localized to dendrites of chordotonal neurons (E). NompA anchors the chordotonal dendrite to the dendritic cap. Para is localized to two segments of the dendrite, the most distal segment overlaps with NompA binding to the distal tip (A). The more proximal region of Para is on the proximal side of the dendrite where NompA is localized, distal to the scaffold protein Eyes-shut (labeled with Mab 21A6; B). This location corresponds to ciliary dilation. The mechanosensitive transient receptor potential (TRP) channels NompC, lav, and Nan are all localized to the dendrites of chordotonal neurons with NompC in the distal region and lav and Nan proximal to the ciliary dilation. Para colocalizes with both NompC and lav (C, D); however, Para is more abundant where NompC is localized. The localization of each protein is summarized in E.

predominantly colocalizes with NompC at the tip of the dendrite (Fig. 5C). Para also partially colocalizes with the more proximal lav (Fig. 5D); however, the majority of Para in dendrites is at the ciliary dilation together with NompC.

Para is required for sound response in the Johnston's organ CNs

Adult flies have a greater sensory repertoire than larvae. Adult flies have more sensitive responses to sound stimuli and have a greater abundance of proprioceptive and

mechanosensitive neurons to maintain complex functions such as flight stabilization and courtship (Currier and Nagel, 2020; Montell, 2021). CNs are essential for hearing in adult *Drosophila* (Eberl et al., 2000). The second antennal segment of the adult fly contains the JO, which consists of 225 scolopidia (Caldwell and Eberl, 2002; Kamikouchi et al., 2006). Each scolopidium contains 2 or three bipolar CNs anchored in antennal segment 2 (Todi et al., 2004). The dendrites are attached to a tubular ECM dendritic cap anchored to the rotating stalk of antennal segment 3 (Todi et al., 2004). The neuron is surrounded by a scolopale cell, a glial-like cell that protects the dendrite and maintains the ionic balance of the extramembrane space of the dendrite (Caldwell and Eberl, 2002; Roy et al., 2013). When sound waves reach the antenna, they cause the stalk to rotate and pull on the dendrites of CNs, opening the mechanosensitive TRP channels NompC, lav, and Nan and initiating a graded potential (Göpfert et al., 2006). The JO develops during pupal stages. Pupae 24–48 h after puparium formation were dissected to observe Para localization and expression. Using *para-T2A-GAL4* driving expression of *UAS-mCD8::GFP*, we do not observe any scolopodia, as labeled by F-Actin, that are not connected to a *para* expressing cell, therefore, like the CN in larvae and embryos, *para* is expressed in all the CNs of the JO (Fig. 6A). This is consistent with the FlyCellAtlas which shows *para* expression in all JO neurons (H. Li et al., 2022). Each scolopodium contains two or three JO neurons that are encased by the F-Actin spindles (Todi et al., 2004). Para is also enriched at the ciliary dilation of the dendrite in JO neurons; however, in each scolopidium, only one Para containing dendrite is observed (Fig. 6B,C; Movie 1). Each scolopodium contains a stereotyped combination of neurons for detecting sound, wind, and gravity respectively (Ishikawa et al., 2020). The restriction of Para localization to just one neuron's dendrite indicates a different physiological role of Na_v channels in different JO neuron types.

To determine whether *para* is essential for CN mechanosensation in the adult JO, we used three RNAi lines (Dietzl et al., 2007) against *para* driven by two separate CN drivers: *atonal-Gal4* (*ato-GAL4*) (Hassan et al., 2000), which drives GAL4 expression in CN precursor cells and the chordotonal lineage, and *tilB-Gal4 nan-GAL4*, which drives GAL4 expression only in CNs (Kim et al., 2003; Kavlie et al., 2010; Roy et al., 2013). All RNAi lines target an exon incorporated into all 60 *para* isoforms ensuring we are not looking at isoform-specific effects (Larkin et al., 2021).

When *para* expression is reduced using any of the three RNAi lines against *para* with either GAL4 driver, the sound-evoked potentials (SEPs) produced in adult female flies in response to computer-generated male courtship pulse song is greatly reduced compared with control animals with no GAL4 driver (Fig. 6D,E; Extended Data Fig. 6-1). Additionally, when *para* expression is reduced, the SEPs in response to pulse stimulation are strongly reduced (Fig. 6D,E). Interestingly a small depolarization can still be detected in the neurons, possibly from the mechanosensitive channels that are remaining (NompC, lav,

Nan). However, when the *para* expression is reduced this signal is severely diminished implicating a role for Para in the excitability of the CN dendrite. Because of the dual nature of Para localization, the reduction in SEPs is likely the result of the loss of *para* in both axons and dendrites. However, we have not been able to isolate the dendrite or axonal-specific functions of Para as we have not been able to remove Para only in dendrites. Attempts were made to inhibit Para using the sodium channel blocker tetrodotoxin, however, we were not able to access the CNs likely because of the glial sheath (Nelson and Laughon, 1993).

Discussion

In *Drosophila*, the composition of ion channels that contribute to the graded potentials in PNS cell dendrites is unclear. Mapping the distribution of Na_v channels in the unipolar neurons of the fly CNS uncovered the SIZ at a DAS (Ravenscroft et al., 2020). Using the same endogenously tagged Para allele, we located the likely SIZ in the multipolar and bipolar neurons of the *Drosophila* PNS. In contrast to the DAS in the unipolar neurons of the fly CNS, the SIZ is at an AIS-like region proximal to the soma in PNS, comparable to the location of the AIS in vertebrate neurons (C.Y.M. Huang and Rasband, 2018). Despite the more proximal location, the SIZ still determines the boundary between the somatodendritic and axonal compartments of the cell. Surprisingly, in addition to the axonal SIZ, a dendritic SIZ, demarcated by the presence of Na_v channels, is present in bipolar CN neurons. The dendritic SIZ is located at the distal tip of the dendrite and overlaps with the localization of the mechanosensitive TRP channels NompC and lav. We believe this is a dendritic SIZ in agreement with a computational model of the crayfish stretch receptors for which Na_v activation is needed to accurately represent *in vivo* recordings (Suslak et al., 2011).

The localization of Para to the CN dendritic SIZ likely explains the TTX-sensitive dendritic spikes previously reported in insect mechanosensitive neurons (Hill, 1983; Oldfield and Hill, 1986; Lehnert et al., 2013; Warren and Matheson, 2018). Two TTX-sensitive spikes occur in the dendrites of locust auditory neurons dendrites. These spikes are recorded in the apical (distal) and basal (proximal) dendrite (Hill, 1983). The basal spikes respond to axonal depolarization and are likely backpropagating APs originating from Para channels opening at the SIZ in the axon. The apical spikes were of unknown origin but are likely to be spikes initiated by Para at the dendritic SIZ. While the dendritic SIZ identified in this study is in the fly and not the locust, Na_v localization is comparable between insect species as indicated by grasshopper Para and *Drosophila* Para having similar localization patterns (H. Wang et al., 2020).

All three identified TRP channels in the CN dendrites, NompC, lav, and Nan, contribute to the mechanotransduction response. Direct patch clamp recordings of lch5 neurons identify a complete loss of mechanotransduction in the absence of lav and Nan, while loss of NompC did not decrease the mechanotransduction response indicating

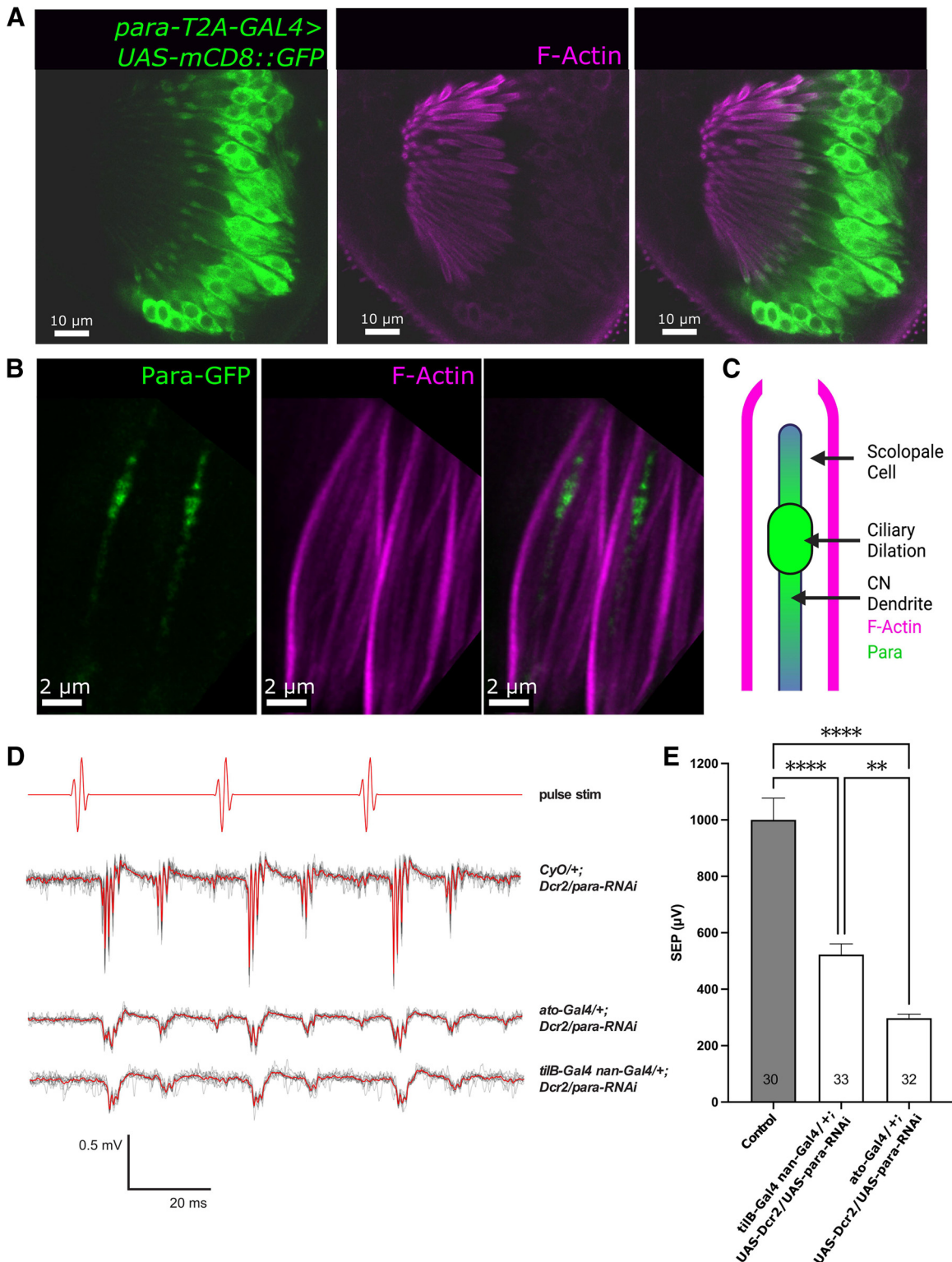


Figure 6. Para is required for sound response in Johnston’s organ (JO). The JO is responsible for detecting auditory stimuli in the adult fly. In the developing pupae, ~54 h after puparium formation *para* is expressed in the chordotonal neurons (CN) of the second antennal segment and not in the support scolopale cells labeled by F-Actin (A). In the chordotonal neurons, Para is localized to the ciliary dilation and distal dendrite of the chordotonal neurons in the JO (B). Diagram depicting the spatial arrangement of Para relative to the sensory cilium and scolopale rods (C). The activity of adult chordotonal neurons can be measured using sound-evoked potentials (SEPs). Acoustic near-field presentation of computer-generated pulse song stimulus (red pulse stim line) evokes strong SEPs in control animals with no Gal-4 driver. Responses to 10 individual stimulus presentations (depicted as light gray lines) are averaged (depicted as red lines; D). RNAi knock-down of *para* using the *ato-Gal4* driver, which drives expression in the chordotonal

continued

sense organ precursor and the resulting chordotonal lineage, or with the *tilB-Gal4 nan-Gal4* driver, which drives expression only in the chordotonal neurons, with Dicer-2 (*Dcr2*) results in a strong reduction in the SEP amplitude (**E**). The SEP of multiple knock-down lines is shown in Extended Data Figure 6-1. Bars and error bars indicate mean \pm SEM, and *Ns* shown within each bar indicate the number of antennae tested. Results of one-way ANOVA with Brown–Forsythe correction and Tukey’s *post hoc* multiple comparisons test are shown (** $p < 0.01$, **** $p < 0.0001$).

that *lav* and *Nan* are the essential channels (B. Li et al., 2021). Patch clamp experiments did uncover that without *NompC* the adaptation time in CNs is a lot shorter (B. Li et al., 2021), therefore the interplay between TRP channels in the dendrites is key for their proper function. The presence of *Para* in the same dendritic space as both *NompC* and *lav* would enable *Para* to facilitate this interaction. It is worth noting, however, that these patch-clamp experiments were performed in conditions where Na_v was inhibited, therefore the electrophysiological interplay between *Para* and the TRP channels remains to be established.

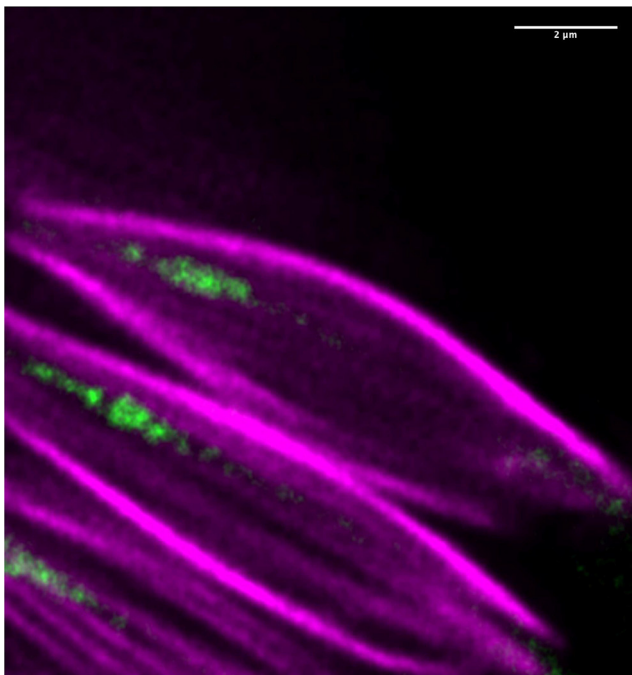
In *Ich5* and *JO* CNs, *Para* is enriched at the ciliary dilation. The ciliary dilation is visible via a bulge in the membrane and is necessary for the separation of the dendrite into distinct regions (E. Lee et al., 2008). Beyond the ciliary dilation’s role in cellular organization, a role in signal transduction has been proposed but how this structure facilitates signal transduction is not clear (Moran et al., 1977; Field and Matheson, 1998). The localization of *Para* to the ciliary dilation is suggestive that Na_v channels may facilitate signal transduction at the ciliary dilation.

TRP channel opening typically occurs in response to mechanical, temperature, chemical, or noxious stimuli (Clapham et al., 2001; Montell et al., 2002; Zheng, 2013; Montell, 2021). However, many TRP channels have been

shown to open in response to voltage (Hofmann et al., 2003; Nilius et al., 2003; Voets et al., 2004; Matta and Ahern, 2007). The rat TRP channels TRPV1 and TRPM8 are hot and cold responsive, respectively (Dhaka et al., 2006); however, under specific conditions, they can open in response to voltage (Voets et al., 2004; Matta and Ahern, 2007). At room temperature and physiological pH, TRPV1 opens at around 0 mV with a half-activation voltage of around 150 mV (Matta and Ahern, 2007). These activation ranges are a lot harder to achieve [compared with the properties of $\text{Na}_v1.2$ (activation ~ -55 mV, half-activation voltage ~ -15 mV; Ogiwara et al., 2009)]. However, for these temperature-sensitive channels when the channel is exposed to higher temperatures the structure of the channel changes, and the half-activation threshold is far lower, -50 mV for TRPV1 at 42°C , which is readily achievable in a sensory neuron (Voets et al., 2004). It is not known whether the fly TRP channels are voltage sensitive, however, the two closest homologs of the vertebrate voltage sensing TRP channel *TRPV1* are *nan* (DIOPT 7/16) and *iav* (5/16; Hu et al., 2011). Interestingly, *iav* and *nan* are only expressed in the chordotonal PNS neuron dendrites where *Para* is localized (Kim et al., 2003; Gong et al., 2004). The possible voltage sensitivity of *lav/Nan* in the same location as a Na_v channel suggests that *Para* activation could influence *lav/Nan* activation or vice versa.

The dendrite of CNs is exposed to stretch forces opening mechanosensitive TRP channels. The presence of *Para* in the CN dendrite imposes the question as to whether *Para* may also be mechanosensitive. Two vertebrate Na_v channels $\text{Na}_v1.4$ (*SCN4A*) and $\text{Na}_v1.5$ (*SCN5A*) that are expressed in contracting muscle tissue have accelerated activation and inactivation kinetics when stretched in *Xenopus* oocytes (Shcherbatko et al., 1999; Tabarean et al., 1999; Morris and Juranka, 2007). While *in vivo* evidence for these channels’ mechanosensitivity is lacking, the G615E mutation in *SCN5A* which predominantly causes long-QT syndrome in patients has normal voltage-gating but aberrant mechanosensitivity indicating a role for $\text{Nav}1.5$ in mechanosensitivity (Strege et al., 2019). While *para* shares homology with *SCN4A* (DIOPT 9/16) and *SCN5A* (DIOPT 11/16; Hu et al., 2011), *para* is not expressed in muscle cells, and evidence for neuronal Na_v channel mechanosensitivity is less obvious (Morris, 2011). *para* has 60 isoforms with different protein sequences and different dynamic properties that likely accommodate the requirements of different neurons (Lin et al., 2009, 2012). An isoform-by-isoform expression study is needed to determine whether the CN *para* isoforms are closer in homology to *SCN5A* and *SCN4A* and thus more likely to be mechanosensitive.

In vertebrate neurons, voltage-gated ion channels can also contribute to graded potentials (Stuart et al.,



Movie 1. *Para* is only present in one Johnston’s Organ neuron per scolopodium. Magenta, F-Actin; green, *Para*-GFP [View online]

1997; Golding and Spruston, 1998; Losonczy and Magee, 2006). In cultured hippocampal CA1 pyramidal neurons and brain slices of rat neocortical pyramidal neurons, spikes in membrane potential are observed in dendrites (Stuart et al., 1997; Losonczy and Magee, 2006; Sun et al., 2014). These dendritic spikes are not affected by the Ca_v channel blocker cadmium but are blocked by the Na_v channel blocker TTX, indicating that they are also generated by Na_v channels (Stuart et al., 1997). In CA1 pyramidal neurons, $Na_v1.6$ is found in the dendrites, but it is 40 times less abundant than it is in axons (Lorincz and Nusser, 2010), while in the dendrites of *Drosophila* CNs, the max intensity of Para is roughly half that seen in the axon (Fig. 4D). Hence, Na_v -dependent dendritic spikes are not an insect-specific phenomenon.

The inner hair cells of humans have a comparable organization to that of the fly CNs (Boekhoff-Falk, 2005). Studies in flies have elucidated key genes and mechanisms of the auditory response in humans (T. Li et al., 2018). One Na_v channel in vertebrates, *SCN8A*, has been implicated in a mouse model of peripheral hearing loss (Mackenzie et al., 2009). Interestingly, dominant variants in *SCN8A* are often implicated with more global neurodevelopmental disorders (Trudeau, 2006; Veeramah et al., 2012). The specific hearing loss identified in the prior mouse studies indicates a specific role in hearing for the affected residue. Na_v localization to the CNs in flies opens the door for the use of *Drosophila* to study the impact of Na_v dysfunction on hearing loss.

While we propose a role for Na_v channels in CN dendrites, the presence of Para in the AIS-like region in addition to the distal dendrites makes the delineation of Para's role in either region impossible with current tools. Reduction of *para* expression using RNAi in the adult JO neurons shows a strong reduction of SEP indicating an inability to process sound. However, we are reducing Para in both the axons and the dendrites and therefore we cannot distinguish whether the loss of Para in dendrites prevents the dendritic depolarization from reaching the soma or whether the axonal AP is lost because of a lack of Para in the AIS. We tried to model dendritic CN activity in *lch5* neurons using GCaMP7 (Dana et al., 2019) and TTX (Pauron et al., 1985) to block sodium channels but were unable to get reliable Na_v channel inhibition, likely because of the insulating glial sheath, and the dynamics of the signal were too fast for reliable separation between axon and dendritic signal. To answer this question new tools are needed to selectively remove proteins in a compartment-specific way.

Para is localized to an AIS-like region in the axons of *Drosophila* PNS neurons. The region of Para localization overlaps with the previously reported AIS-like region in multipolar *ddaE* neurons, identified by an accumulation of over-expressed *Ank2*, *Shal*, and *Elk* and a diffusion barrier akin to the one seen at the vertebrate AIS (Jegla et al., 2016). The localization of Para and the *AnkG* homolog *Ank2* in the AIS-like region of the PNS is of note as the *AnkG* binding motif in Na_v channels is not present in *para* indicating an alternative binding site and/or clustering mechanism in the fly PNS AIS-like region (Jegla et al., 2016).

In this study, we have identified the likely SIZ(s) in the multipolar and bipolar neurons of the fly PNS through the characterization of Na_v channel distribution. We have confirmed the presence of an axonal SIZ at an AIS-like region and surprisingly identified a likely dendritic SIZ in CNs throughout *Drosophila* development. The presence of Na_v channels in a dendritic and axonal SIZ in the fly PNS introduces an accessible system for further study into the role of Na_v channels in how animals sense their environment.

References

- Ainsley JA, Pettus JM, Bosenko D, Gerstein CE, Zinkevich N, Anderson MG, Adams CM, Welsh MJ, Johnson WA (2003) Enhanced locomotion caused by loss of the *Drosophila* DEG/ENaC protein Pickpocket1. *Curr Biol* 13:1557–1563.
- Akitake B, Ren Q, Boiko N, Ni J, Sokabe T, Stockand JD, Eaton BA, Montell C (2015) Coordination and fine motor control depend on *Drosophila* TRP γ . *Nat Commun* 6:7288.
- Blochlinger K, Jan LY, Jan YN (1991) Transformation of sensory organ identity by ectopic expression of Cut in *Drosophila*. *Genes Dev* 5:1124–1135.
- Bodmer R, Jan YN (1987) Morphological differentiation of the embryonic peripheral neurons in *Drosophila*. *Roux Arch Dev Biol* 196:69–77.
- Boekhoff-Falk G (2005) Hearing in *Drosophila*: development of Johnston's organ and emerging parallels to vertebrate ear development. *Dev Dyn* 232:550–558.
- Caldwell JC, Eberl DF (2002) Towards a molecular understanding of *Drosophila* hearing. *J Neurobiol* 53:172–189.
- Carlson SD, Hilgers SL, Juang JL (1997) Ultrastructure and blood-nerve barrier of chordotonal organs in the *Drosophila* embryo. *J Neurocytol* 26:377–388.
- Cheng LE, Song W, Looger LL, Jan LY, Jan YN (2010) The role of the TRP channel NompC in *Drosophila* larval and adult locomotion. *Neuron* 67:373–380.
- Chung YD, Zhu J, Han Y-G, Kernan MJ (2001) *nompA* encodes a PNS-specific, ZP domain protein required to connect mechanosensory dendrites to sensory structures. *Neuron* 29:415–428.
- Clapham DE, Runnels LW, Strübing C (2001) The TRP ion channel family. *Nat Rev Neurosci* 2:387–396.
- Cosens DJ, Manning A (1969) Abnormal electroretinogram from a *Drosophila* mutant. *Nature* 224:285–287.
- Currier TA, Nagel KI (2020) Multisensory control of navigation in the fruit fly. *Curr Opin Neurobiol* 64:10–16.
- Dana H, Sun Y, Mohar B, Hulse BK, Kerlin AM, Hasseman JP, Tsegaye G, Tsang A, Wong A, Patel R, Macklin JJ, Chen Y, Konnerth A, Jayaraman V, Looger LL, Schreier ER, Svoboda K, Kim DS (2019) High-performance calcium sensors for imaging activity in neuronal populations and microcompartments. *Nat Methods* 16:649–657.
- Dhaka A, Viswanath V, Patapoutian A (2006) TRP ion channels and temperature sensation. *Annu Rev Neurosci* 29:135–161.
- Dietzl G, Chen D, Schnorrer F, Su K-C, Barinova Y, Fellner M, Gasser B, Kinsey K, Oettel S, Scheiblauer S, Couto A, Marra V, Keleman K, Dickson BJ (2007) A genome-wide transgenic RNAi library for conditional gene inactivation in *Drosophila*. *Nature* 448:151–156.
- Eberl DF, Kernan MJ (2011) Recording sound-evoked potentials from the *Drosophila* antennal nerve. *Cold Spring Harb Protoc* 2011:prot5576.
- Eberl DF, Hardy RW, Kernan MJ (2000) Genetically similar transduction mechanisms for touch and hearing in *Drosophila*. *J Neurosci* 20:5981–5988.
- Evans CJ, Olson JM, Ngo KT, Kim E, Lee NE, Kuoy E, Patananan AN, Sitz D, Tran P, Do M-T, Yackle K, Cespedes A, Hartenstein V, Call GB, Banerjee U (2009) G-TRACE: rapid Gal4-based cell lineage analysis in *Drosophila*. *Nat Methods* 6:603–605.

- Field LH, Matheson T (1998) Chordotonal organs of insects. *Adv In Insect Phys* 27:1–56.
- Fujita SC, Zipursky SL, Benzer S, Ferrús A, Shotwell SL (1982) Monoclonal antibodies against the *Drosophila* nervous system. *Proc Natl Acad Sci USA* 79:7929–7933.
- George AL, David Ledbetter H, Kallen RG, Barchi RL (1991) Assignment of a human skeletal muscle sodium channel α -subunit gene (SCN4A) to 17q23.1–25.3. *Genomics* 9:555–556.
- Gohl DM, Silies MA, Gao XJ, Bhalarao S, Luongo FJ, Lin C-C, Potter CJ, Clandinin TR (2011) A versatile in vivo system for directed dissection of gene expression patterns. *Nat Methods* 8:231–237.
- Golding NL, Spruston N (1998) Dendritic sodium spikes are variable triggers of axonal action potentials in hippocampal CA1 pyramidal neurons. *Neuron* 21:1189–1200.
- Gong Z, Son W, Chung YD, Kim J, Shin DW, McClung CA, Lee Y, Lee HW, Chang D-J, Kaang B-K, Cho H, Oh U, Hirsh J, Kernan MJ, Kim C (2004) Two interdependent TRPV channel subunits, inactive and nanchung, mediate hearing in *Drosophila*. *J Neurosci* 24:9059–9066.
- Göpfert MC, Albert JT, Nadrowski B, Kamikouchi A (2006) Specification of auditory sensitivity by *Drosophila* TRP channels. *Nat Neurosci* 9:999–1000.
- Grueber WB, Graubard K, Truman JW (2001) Tiling of the body wall by multidendritic sensory neurons in *manduca sexta*. *J Comp Neurol* 440:271–283.
- Grueber WB, Jan LY, Jan YN (2003) Different levels of the homeodomain protein cut regulate distinct dendrite branching patterns of *Drosophila* multidendritic neurons. *Cell* 112:805–818.
- Hartenstein V (1988) Development of *Drosophila* larval sensory organs: spatiotemporal pattern of sensory neurones, peripheral axonal pathways and sensilla differentiation. *Development* 102:869–886.
- Hassan BA, Bermingham NA, He Y, Sun Y, Jan Y-N, Zoghbi HY, Bellen HJ (2000) Atonal regulates neurite arborization but does not act as a proneural gene in the *Drosophila* brain. *Neuron* 25:549–561.
- Hill KG (1983) The physiology of locust auditory receptors. *J Comp Physiol* 152:483–493.
- Hofmann T, Chubananov V, Gudermann T, Montell C (2003) TRPM5 is a voltage-modulated and Ca²⁺-activated monovalent selective cation channel. *Curr Biol* 13:1153–1158.
- Hong C, Ganetzky B (1994) Spatial and temporal expression patterns of two sodium channel genes in *Drosophila*. *J Neurosci* 14:5160–5169.
- Hu Y, Flockhart I, Vinayagam A, Bergwitz C, Berger B, Perrimon N, Mohr SE (2011) An integrative approach to ortholog prediction for disease-focused and other functional studies. *BMC Bioinformatics* 12:357.
- Huang CYM, Rasband MN (2018) Axon initial segments: structure, function, and disease. *Ann N Y Acad Sci* 1420:46–61.
- Huang J, Zhou W, Watson AM, Jan Y-N, Hong Y (2008) Efficient ends-out gene targeting in *Drosophila*. *Genetics* 180:703–707.
- Husain N, Pellikka M, Hong H, Klimentova T, Choe KM, Clandinin T, Tepass U (2006) The Agrin/Perlecan-related protein eyes shut is essential for epithelial lumen formation in the *Drosophila* retina. *Dev Cell* 11:483–493.
- Ishikawa Y, Fujiwara M, Wong J, Ura A, Kamikouchi A (2020) Stereotyped combination of hearing and wind/gravity-sensing neurons in the Johnston's organ of *Drosophila*. *Front Physiol* 10:1552.
- Jarman AP, Grau Y, Jan LY, Jan YN (1993) atonal is a proneural gene that directs chordotonal organ formation in the *Drosophila* peripheral nervous system. *Cell* 73:1307–1321.
- Jegla T, Nguyen MM, Feng C, Goetschius DJ, Luna E, van Rossum DB, Kamel B, Pisupati A, Milner ES, Rolls MM (2016) Bilateral giant ankyrins have a common evolutionary origin and play a conserved role in patterning the axon initial segment. *PLoS Genet* 12:e1006457.
- Kamikouchi A, Shimada T, Ito K (2006) Comprehensive classification of the auditory sensory projections in the brain of the fruit fly *Drosophila melanogaster*. *J Comp Neurol* 499:317–356.
- Kavlie RG, Kernan MJ, Eberl DF (2010) Hearing in *Drosophila* requires TilB, a conserved protein associated with ciliary motility. *Genetics* 185:177–188.
- Kim J, Chung YD, Park D, Choi S, Shin DW, Soh H, Lee HW, Son W, Yim J, Park C-S, Kernan MJ, Kim C (2003) A TRPV family ion channel required for hearing in *Drosophila*. *Nature* 424:81–84.
- Larkin A, Marygold SJ, Antonazzo G, Attrill H, Dos Santos G, Garapati PV, Goodman JL, Gramates LS, Millburn G, Strelets VB, Tabone CJ, Thurmond J; FlyBase Consortium (2021) FlyBase: updates to the *Drosophila melanogaster* knowledge base. *Nucleic Acids Res* 49:D899–D907.
- Lee E, Sivan-Loukianova E, Eberl DF, Kernan MJ (2008) An IFT-A protein is required to delimit functionally distinct zones in mechanosensory cilia. *Curr Biol* 18:1899–1906.
- Lee J, Moon S, Cha Y, Chung YD (2010) *Drosophila* TRPN (= NOMPC) channel localizes to the distal end of mechanosensory cilia. *PLoS One* 5:e11012.
- Lee PT, et al. (2018) A gene-specific T2A-GAL4 library for *Drosophila*. *Elife* 7:e35574.
- Lehnert BP, Baker AE, Gaudry Q, Chiang A-S, Wilson RI (2013) Distinct roles of TRP channels in auditory transduction and amplification in *Drosophila*. *Neuron* 77:115–128.
- Li B, Li S, Zheng H, Yan Z (2021) Nanchung and inactive define pore properties of the native auditory transduction channel in *Drosophila*. *Proc Natl Acad Sci USA* 118:e2106459118.
- Li H, et al. (2022) Fly cell atlas: a single-nucleus transcriptomic atlas of the adult fruit fly. *Science* 375:eabk2432.
- Li T, Giagtzoglou N, Eberl DF, Jaiswal SN, Cai T, Godt D, Groves AK, Bellen HJ (2016) The E3 ligase Ubr3 regulates Usher syndrome and MYH9 disorder proteins in the auditory organs of *Drosophila* and mammals. *Elife* 5:e15258.
- Li T, Bellen HJ, Groves AK (2018) Using *Drosophila* to study mechanisms of hereditary hearing loss. *Dis Model Mech* 11:dmm031492.
- Liang X, Madrid J, Saleh HS, Howard J (2011) NOMPC, a member of the TRP channel family, localizes to the tubular body and distal cilium of *Drosophila* campaniform and chordotonal receptor cells. *Cytoskeleton (Hoboken)* 68:1–7.
- Lin WH, Wright DE, Muraro NI, Baines RA (2009) Alternative splicing in the voltage-gated sodium channel DmNa_v regulates activation, inactivation, and persistent current. *J Neurophysiol* 102:1994–2006.
- Lin WH, Günay C, Marley R, Prinz AA, Baines RA (2012) Activity-dependent alternative splicing increases persistent sodium current and promotes seizure. *J Neurosci* 32:7267–7277.
- Liu L, Yermolaieva O, Johnson WA, Abboud FM, Welsh MJ (2003) Identification and function of thermosensory neurons in *Drosophila* larvae. *Nat Neurosci* 6:267–273.
- Lorincz A, Nusser Z (2010) Molecular identity of dendritic voltage-gated sodium channels. *Science* 328:906–909.
- Losonczy A, Magee JC (2006) Integrative properties of radial oblique dendrites in hippocampal CA1 pyramidal neurons. *Neuron* 50:291–307.
- Mackenzie FE, Parker A, Parkinson NJ, Oliver PL, Brooker D, Underhill P, Lukashkina VA, Lukashkin AN, Holmes C, Brown SDM (2009) Analysis of the mouse mutant Cloth-ears shows a role for the voltage-gated sodium channel Scn8a in peripheral neural hearing loss. *Genes Brain Behav* 8:699–713.
- Matta JA, Ahern GP (2007) Voltage is a partial activator of rat thermosensitive TRP channels. *J Physiol* 585:469–482.
- Montell C (2021) *Drosophila* sensory receptors—a set of molecular Swiss Army Knives. *Genetics* 217:1–34.
- Montell C, Birnbaumer L, Flockerzi V, Bindels RJ, Bruford EA, Caterina MJ, Clapham DE, Harteneck C, Heller S, Julius D, Kojima I, Mori Y, Penner R, Prawitt D, Scharenberg AM, Schultz G, Shimizu N, Zhu MX (2002) A unified nomenclature for the superfamily of TRP cation channels. *Mol Cell* 9:229–231.
- Moran DT, Varela FJ, Rowley JC 3rd (1977) Evidence for active role of cilia in sensory transduction. *Proc Natl Acad Sci USA* 74:793–797.
- Morris CE (2011) Voltage-gated channel mechanosensitivity: fact or friction? *Front Physiol* 2:25.
- Morris CE, Juranka PF (2007) Nav channel mechanosensitivity: activation and inactivation accelerate reversibly with stretch. *Biophys J* 93:822–833.

- Nelson HB, Laughon A (1993) *Drosophila* glial architecture and development: analysis using a collection of new cell specific markers. *Roux Arch Dev Biol* 202:341–354.
- Nilius B, Prenen J, Droogmans G, Voets T, Vennekens R, Freichel M, Wissenbach U, Flockerzi V (2003) Voltage dependence of the Ca²⁺-activated cation channel TRPM4. *J Biol Chem* 278:30813–30820.
- Ogiwara I, Ito K, Sawaishi Y, Osaka H, Mazaki E, Inoue I, Montal M, Hashikawa T, Shike T, Fujiwara T, Inoue Y, Kaneda M, Yamakawa K (2009) De novo mutations of voltage-gated sodium channel II gene SCN2A in intractable epilepsies. *Neurology* 73:1046–1053.
- Oldfield BP, Hill KG (1986) Functional organization of insect auditory sensilla. *J Comp Physiol* 158:27–34.
- Orogozo V, Grueber WB (2005) FlyPNS, a database of the *Drosophila* embryonic and larval peripheral nervous system. *BMC Dev Biol* 5:4.
- Pauron D, Barhanian J, Lazdunski M (1985) The voltage-dependent Na⁺ channel of insect nervous system identified by receptor sites for tetrodotoxin, and scorpion and sea anemone toxins. *Biochem Biophys Res Commun* 131:1226–1233.
- Pfeiffer BD, Ngo TTB, Hibbard KL, Murphy C, Jenett A, Truman JW, Rubin GM (2010) Refinement of tools for targeted gene expression in *Drosophila*. *Genetics* 186:735–755.
- Ravenscroft TA, Janssens J, Lee PT, Tepe B, Marcogliese PC, Makhzami S, Holmes TC, Aerts S, Bellen HJ (2020) *Drosophila* voltage-gated sodium channels are only expressed in active neurons and are localized to distal axonal initial segment-like domains. *J Neurosci* 40:7999–8024.
- Rothwell WF, Sullivan W (2007) Fixation of *Drosophila* embryos. *Cold Spring Harb Protoc* 2007:pdb.prot4827.
- Roy M, Sivan-Loukianova E, Eberl DF (2013) Cell-type-specific roles of Na⁺/K⁺ ATPase subunits in *Drosophila* auditory mechanosensation. *Proc Natl Acad Sci U S A* 110:181–186.
- Schrader S, Merritt DJ (2000) Central projections of *Drosophila* sensory neurons in the transition from embryo to larva. *J Comp Neurol* 425:34–44.
- Schrader S, Merritt DJ (2007) Dorsal longitudinal stretch receptor of *Drosophila melanogaster* larva – Fine structure and maturation. *Arthropod Struct Dev* 36:157–169.
- Shcherbatko A, Ono F, Mandel G, Brehm P (1999) Voltage-dependent sodium channel function is regulated through membrane mechanics. *Biophys J* 77:1945–1959.
- Shearin HK, Macdonald IS, Spector LP, Stowers RS (2014) Hexameric GFP and mCherry reporters for the *Drosophila* GAL4, Q, and LexA transcription systems. *Genetics* 196:951–960.
- Singhania A, Grueber WB (2014) Development of the embryonic and larval peripheral nervous system of *Drosophila*. *Wiley Interdiscip Rev Dev Biol* 3:193–210.
- Stocker RF (1994) The organization of the chemosensory system in *Drosophila melanogaster*: a review. *Cell Tissue Res* 275:3–26.
- Strege PR, Mercado-Perez A, Mazzone A, Saito YA, Bernard CE, Farrugia G, Beyder A (2019) SCN5A mutation G615E results in Nav1.5 voltage-gated sodium channels with normal voltage-dependent function yet loss of mechanosensitivity. *Channels (Austin)* 13:287–298.
- Stuart G, Schiller J, Sakmann B (1997) Action potential initiation and propagation in rat neocortical pyramidal neurons. *J Physiol* 505:617–632.
- Sun Q, Srinivas KV, Sotayo A, Siegelbaum SA (2014) Dendritic Na⁺ spikes enable cortical input to drive action potential output from hippocampal CA2 pyramidal neurons. *Elife* 3:e04551.
- Suslak TJ, Armstrong JD, Jarman AP (2011) A general mathematical model of transduction events in mechano-sensory stretch receptors. *Network* 22:133–142.
- Suslak TJ, Watson S, Thompson KJ, Shenton FC, Bewick GS, Armstrong JD, Jarman AP (2015) Piezo is essential for amiloride-sensitive stretch-activated mechanotransduction in larval *Drosophila* dorsal bipolar dendritic sensory neurons. *PLoS One* 10:e0130969.
- Suzuki DT, Grigliatti T, Williamson R (1971) Temperature-sensitive mutations in *Drosophila melanogaster*. VII. A mutation (para-ts) causing reversible adult paralysis. *Proc Natl Acad Sci USA* 68:890–893.
- Swerup C, Rydqvist B (1996) A mathematical model of the crustacean stretch receptor neuron. Biomechanics of the receptor muscle, mechanosensitive ion channels, and macrotransducer properties. *J Neurophysiol* 76:2211–2220.
- Tabarean IV, Juranka P, Morris CE (1999) Membrane stretch affects gating modes of a skeletal muscle sodium channel. *Biophys J* 77:758–774.
- Todi SV, Sharma Y, Eberl DF (2004) Anatomical and molecular design of the *Drosophila* antenna as a flagellar auditory organ. *Microsc Res Tech* 63:388–399.
- Tracey WD, Wilson RI, Laurent G, Benzer S (2003) painless, a *Drosophila* gene essential for nociception. *Cell* 113:261–273.
- Trudeau MM, Dalton JC, Day JW, Ranum LPW, Meisler MH (2006) Heterozygosity for a protein truncation mutation of sodium channel SCN8A in a patient with cerebellar atrophy, ataxia, and mental retardation. *J Med Genet* 43:527–530.
- Tsubouchi A, Caldwell JC, Tracey WD (2012) Dendritic filopodia, ripped pocket, NOMPC, and NMDARs contribute to the sense of touch in *Drosophila* larvae. *Curr Biol* 22:2124–2134.
- Veeramah KR, O'Brien JE, Meisler MH, Cheng X, Dib-Hajj SD, Waxman SG, Talwar D, Girirajan S, Eichler EE, Restifo LL, Erickson RP, Hammer MF (2012) De novo pathogenic SCN8A mutation identified by whole-genome sequencing of a family quartet affected by infantile epileptic encephalopathy and SUDEP. *Am J Hum Genet* 90:502–510.
- Venken KJT, Schulze KL, Haelterman NA, Pan H, He Y, Evans-Holm M, Carlson JW, Levis RW, Spradling AC, Hoskins RA, Bellen HJ (2011) MIMIC: a highly versatile transposon insertion resource for engineering *Drosophila melanogaster* genes. *Nat Methods* 8:737–743.
- Vervoort M, Merritt DJ, Ghysen A, Dambly-Chaudière C (1997) Genetic basis of the formation and identity of type I and type II neurons in *Drosophila* embryos. *Development* 124:2819–2828.
- Voets T, Droogmans G, Wissenbach U, Janssens A, Flockerzi V, Nilius B (2004) The principle of temperature-dependent gating in cold- and heat-sensitive TRP channels. *Nature* 430:748–754.
- Wang H, Foquet B, Dewell RB, Song H, Dierick HA, Gabbiani F (2020) Molecular characterization and distribution of the voltage-gated sodium channel, Para, in the brain of the grasshopper and vinegar fly. *J Comp Physiol A Neuroethol Sens Neural Behav Physiol* 206:289–307.
- Wang X, Zhang MW, Kim JH, Macara AM, Sterne G, Yang T, Ye B (2015) The Krüppel-like factor Dar1 determines multipolar neuron morphology. *J Neurosci* 35:14251–14259.
- Warren B, Matheson T (2018) The role of the mechanotransduction ion channel candidate Nanchung-Inactive in auditory transduction in an insect ear. *J Neurosci* 38:3741–3752.
- Zhang W, Yan Z, Jan LY, Jan YN (2013) Sound response mediated by the TRP channels NOMPC, NANCHUNG, and INACTIVE in chordotonal organs of *Drosophila* larvae. *Proc Natl Acad Sci USA* 110:13612–13617.
- Zheng J (2013). Molecular mechanism of TRP channels. *Compr Physiol* 3:221–242.
- Zhong L, Hwang RY, Tracey WD (2010) Pickpocket is a DEG/ENaC protein required for mechanical nociception in *Drosophila* larvae. *Curr Biol* 20:429–434.